

Cerium Modified Pillared Montmorillonite Supported Cobalt Catalysts for Fischer Tropsch Synthesis

¹Nisar Ahmad*, ¹Zulfiqar Ali, ²Nisar Ali, ³Naeem Shahzad

⁴Fida Hussain, and ¹Syed Mustansar Abbas

¹Nanoscience and Catalysis Division, National Centre for Physics, QAU Campus, Islamabad, 43520, Pakistan.

²Department of Physics, Government Postgraduate Jehan Zaib College, Saidu Sharif, Swat, Pakistan.

³National University of Science and Technology, Islamabad.

⁴School of Resources and Environmental Engineering, Wuhan University of Technology, China.

nisar_shawar@yahoo.com, nisarchemist@gmail.com*

(Received on 18th September 2014, accepted in revised form 27th April 2015)

Summary: Fischer-Tropsch (FT) synthesis was accomplished over Al-pillared Montmorillonite supported 20 wt% Co modified with different weight% of cerium catalysts. These catalysts were prepared by impregnation method while structural characterizations of the prepared samples were performed by XRD, TPR, NH₃TPD, TGA, BET, XRF and SEM techniques. The Fischer Tropsch reaction was studied in fixed bed micro catalytic reactor at temperature range of 220, 260 and 275 °C and at different pressure (1, 5, and 10 bars). From the activity results, it was found that by pillaring NaMMT with Al higher catalytic activity and lower methane selectivity of NaMMT was achieved. Furthermore, the results of FT synthesis reaction revealed that cerium incorporation increased the dispersion of Co₃O₄ on the surface and consequently resulted in enhanced catalytic activity. Additionally, the C₅-C₁₂ hydrocarbons and methane selectivity increased while C₂₂₊ hydrocarbons selectivity was decreased over cerium modified catalysts. Higher reaction temperature (>220 °C) resulted in significant enhancement in CO conversion and methane selectivity. Though, increase in pressure from 1 to 10 bars eventually resulted in increase in C₅₊ hydrocarbons and decrease in methane and C₂-C₅ hydrocarbons selectivity.

Key Words: FT synthesis; Syngas; Cobalt; Cerium; Hydrocarbons; Montmorillonite

Introduction

Fischer-Tropsch (FT) synthesis is an industrially well-known important process which deals with the conversion of syngas (H₂/CO) into value added products. For this purpose, a variety of supported transition metal catalysts containing cobalt, iron and ruthenium have been extensively studied due to higher catalytic activity [1]. Among them, cobalt have been preferred due the lower methane and higher C₅₊ hydrocarbons selectivity at high pressure and lower temperature [2].

The use of Co-based catalysts has attained considerable attention due to lower temperature FT synthesis [3] but the major drawback is the formation of higher molecular weight hydrocarbons (waxes) which result in blocking active sites of the catalyst and hence lowering of catalytic activity. The FT synthesis products over Co-based catalysts consist of multi component mixture of linear and branched hydrocarbons and oxygenated compounds. The hydrocarbons in the range of C₂₂₊ are called FT waxes, having higher boiling point and remain solid at lower temperature. Considerable progresses have been made towards the cracking of these higher hydrocarbon fractions to lower ones, in order to increase the overall conversion and selectivity of liquid hydrocarbons in FT synthesis. It was found that the active metals along with supports play an important role in FT synthesis that effect the activity

and products selectivity of a catalysts dramatically [4, 5]. Recent studies showed that silica, alumina, titania and zeolite are the most extensively used supports in FT synthesis [4, 6]. However, considerable attention has been paid towards the use of bifunctional catalysts for the hydrocracking of long chain alkanes. Transition metals such as Co, Ni, Pt, Pd and bimetallic Ni/Co alloy systems have been extensively used over acidic supports such as ZSM-5, ZSM-22, mordenite, SAPO-31, SAPO-11, SAPO-41 for the hydrocracking of higher molecular weight hydrocarbon waxes. In active metal support systems, the role of acidic support is hydrocracking and hydroisomerization while transition metal provides a site of hydrogenation and dehydrogenation [7, 8].

It has been reported that Montmorillonite (MMT) clay has been widely used for hydrocracking catalysts in the petroleum industries as a support due its similar properties to those of zeolite [9, 10]. But the major drawback associated with MMT is its lower thermal stability and lower porosity which can be improved by modification or pillaring of MMT [11]. Various methods has been employed for fabrication of Pillared montmorillonite (PILC) and one of them includes the exchange of cations of MMT with larger cations through the hydrolysis of metal salts or oxides. The hydrolysis process results

*To whom all correspondence should be addressed.

into the formation of larger sized cations which can replace or exchange the cations already present in the interlayer of MMT [12]. Previously, the effect of MMT as a support for the iron FT catalyst have been explored but the main problem associated with this system is the production of unwanted products (methane and carbon dioxide etc) due to the complexity of metal oxide reduction to metallic state by MMT [13]. So, there is an essential need to develop a catalyst with minimum production of methane and CO₂. For this purpose, it is scrutinized that the use of MMT supported Co catalyst could result in increase of C₂-C₁₂ hydrocarbons selectivity and decrease in selectivity of C₂₁₊ hydrocarbons due to the cracking ability of MMT.

Furthermore, use of certain promoters with MMT supported catalyst can notably decrease the higher selectivity of CO₂ and methane. Various metal promoters like Re, Pt and Ru and oxides promoters including ZrO₂, CeO₂ and La₂O₃ have been explored to increase catalytic activity and C₅₊ products selectivity of cobalt based FT catalysts [14-21]. Previously, CeO-Co/C has been reported as an efficient catalyst resulting in the lower methane, higher olefins and heavy hydrocarbons selectivity in the FT synthesis [20, 22]. The partial reduction of CeO₂ results in the CO adsorption sites which are responsible for enhanced CO dissociation [20]. Until now, little literature is available on the MMT supported cobalt catalysts for enhanced gasoline selectivity including hydrocarbons via hydrocracking of FT waxes. In current study the FT activity of MMT supported cobalt catalyst have been investigated thoroughly. Furthermore, effect of different cerium incorporations on the activity and product selectivity has been explored during FT synthesis.

Experimental

Materials

Sodium Montmorillonite (NaMMT), Aluminium chloride (AlCl₃ .6H₂O) and cobalt nitrate (Co(NO₃)₂.6H₂O) from Sigma Aldrich while Cerium nitrate (Ce(NO₃)₃.6H₂O) from Merck were of analytical grade and were used without any further purification. NaMMT was selected as a starting material to prepare Al-PILC.

Preparation of Al-PILC and 20 wt% Co/Al-PILC

The Al-PILC and 20 wt% Co/Al-PILC were synthesized by our already reported method [4, 9].

Preparation of 20 wt% Co/Al-PILC with different Ce-loadings

Ce-Co/Al-PILC with 20 wt% Co containing 0.5, 1.0, 1.6 wt% Ce-loadings was prepared by wet impregnation method. The required amount of calcined pillared clay was dispersed into 0.1M solution of Co(NO₃)₂.6H₂O and Ce(NO₃)₃.6H₂O with constant stirring. The resultant suspension was evaporated at 40 °C through rotary evaporator, washed with distilled water, dried and calcined at 400 °C for 5h.

Characterization of Prepared Catalysts

The structural parameters of the prepared samples have been evaluated by X-ray diffraction (XRD) using Scintag XDS 2000 diffractometer. Textural parameters including BET surface area and pore volume have been acquired by Coulter SA 3100 analyzer using liquid nitrogen at a temperature of (78 K). H₂-TPR and NH₃-TPD profile was recorded on a TPDRO/1100 Series. Thermo gravimetric analyses (TGA) of all catalysts were carried out on Thermo Electron Corporation, Italy. Mettler TGA/SDTA 851e in the temperature range of 0-100 °C. Chemical composition and catalysts surface morphology was studied by SEM JEOL JSM 6490-A equipped with Energy Dispersive X-ray Spectrometer (EDX). JEOL Model JSX-3202M X-ray fluorescence was used for chemical composition determination.

Catalyst Evaluations

The catalytic activity was conducted in a fixed bed micro reactor. The detailed procedure and setup for catalytic activity evaluation is described in our previously reported work [4, 9, 11].

Results and Discussion

Chemical Composition Analysis

The chemical composition of the naturally occurring clay NaMMT and our prepared samples i.e., Al-PILC and Ce-Co /Al-PILC was determined through XRF and given in Table-1.

Table-1: Chemical composition (wt%) of the prepared catalysts determined by XRF analysis.

Samples	SiO ₂	Al ₂ O ₃	Na ₂ O	Fe ₂ O ₃	MgO	Co ₂ O ₃	CeO ₂
NaMMT	55.6	30.3	4.41	2.3	5.3	-	-
Al-PILC	53.1	40.4	<0.001	0.9	5.1	-	-
0.5 Ce -Co/Al-PILC	39.9	34.0	<0.001	0.8	5.1	19.3	0.8
1.0 Ce -Co/Al-PILC	39.3	33.9	<0.001	0.8	5.1	19.6	1.0
1.6 Ce-Co/Al-PILC	39.0	34.2	<0.001	0.8	5.1	18.5	1.7

It is obvious from the Table-1 that there is an increase in Al_2O_3 content of the clay from 30.1 to 40.4 which can be attributed to the complete substitution of Na cation present in MMT interlayer by Al_2O_3 . However, Mg and SiO_2 contents are almost same for all the Co-loaded MMT samples depicting no obvious change in the clay sheets composition.

XRD Characterization

The XRD pattern of NaMMT and AlPILC is already described in our previous work [9]. Fig. 1 shows the XRD pattern of Ce-Co/Al-PILC. After pillaring of MMT with Al which replace the smaller cation in the interlayer of two dimensional MMT structure causes change in the gallery height and d_{001} basal plane [23]. As can be seen in Fig. 1, there is an intense peak at $2\theta = 8^\circ$ with basal reflection of 001, basal spacing of 12.06 Å and a host layer thickness of 9.3 Å. Gallery height of 3.3 Å was calculated by subtracting the host layer thickness from the obtained basal spacing of the NaMMT which is similar to the previously reported value [23]. The XRD spectra of Al-PILC gives diffraction planes at 8° , 19.7° , 35° and 61.8° which are characteristic of two dimensional layers structure of clay [24]. The Al-PILC gives the 001 basal reflection at lower 2θ value with increased d-spacing values i.e., from 12.06 to 18.7 Å and increased gallery height i.e., from 3.3 to 9.4 Å. This effect may be due to the expansion of MMT layer structure as a consequence of pillaring which was similar to the reported value [9]. However, the decrease in intensity of 001 peak of Al-PILC can be attributed to the intercalation of Al into the MMT clay interlayers. Moreover, no other structural changes or shifting of peak positions were observed in the XRD spectra of both the samples.

The presence of 001 diffraction peak, a basal reflection of Al-PILC is evident from the XRD pattern of Ce-Co/Al-PILC catalysts as shown in Fig. 1. While the small decrease in the 001 diffraction peak intensity was observed corresponding to the slight decrease in layered structure of MMT. XRD pattern of Ce-Co/ Al-PILC (Fig. 1) shows cobalt oxides (Co_3O_4) diffraction peaks at 19.5° , 31.4° , 36.9° , 44.9° and 59.6° (JCPDS 65-3103) in all samples indicating a uniform dispersion of pure Co_3O_4 on pillared MMT [25]. While no reflection peaks were observed for cerium in all samples thus confirming the high dispersion and lower content of cerium on Al-PILC surface [26].

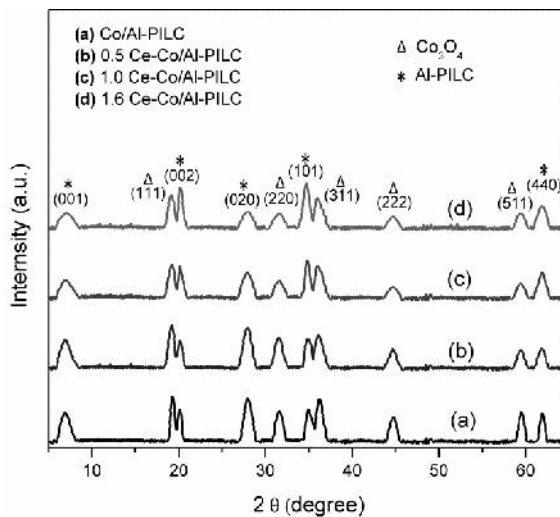


Fig. 1: XRD pattern of the samples.

The average crystallite size of the Co_3O_4 was determined by employing the Scherrer equation and was found in the range of 30-40 nm. Furthermore, no reflection planes of cobalt aluminates or silicate in the XRD pattern were found, showing the presence of highly dispersed Co_3O_4 . This also confirms that no interaction of Co with MMT components exists [25-28].

Textural Properties of Ce-Co/Al-PILC

The textural data including BET surface area pore volume and pore diameter are summarized in Table-2. The higher surface area of Al-PILC as compared to NaMMT indicates that Al has successfully replaced Na^+ present in the silicate layer of MMT. The larger surface area is due to the higher N_2 adsorption as a result of increased pore volume caused by Al-pillaring [25]. While the addition of cerium and Co on Al-PILC resulted in decrease in BET surface area and pore volume which can be attributed to the presence of metal particles at pore openings and on the surface of the pores. Since, the average pore diameter and pore size remained constant for all samples, therefore the pore blocking of Co can be neglected [10]. The pore volume depicts the micro porous and non-porous nature of Ce-Co/Al-PILC and NaMMT, respectively.

Table-2: Textural properties of the prepared catalysts.

Sample	BET (m^2/g)	Pore diameter (Å)	Pore volume (cm^3/g)
Na MMT	39.2	4.8	0.08
Al-PILC	254.0	14.6	0.20
0.5 Ce-Co/Al-PILC	229.0	12.2	0.19
1.0 Ce-Co/Al-PILC	225.0	11.0	0.18
1.6 Ce-Co/Al-PILC	222.0	10.3	0.19

Acidic Property

NH_3 -TPD study was carried out for the evaluation of acidic properties of the prepared sample. It is obvious from NH_3 -TPD profile as shown in Fig. 2, that Al-PILC possess both Bronsted and Lewis acidic sites [29]. The lower temperature desorption peak at 150 °C and higher temperature desorption peak at 600 °C can be attributed to weaker Bronsted acidic and stronger Lewis acidic site respectively. The lower temperature desorption peak (at 150 °C, Bronsted site) of Al-PILC is due to the presence of hydroxyl groups in the layered structure of MMT [30]. However, the high temperature desorption (600 °C) for strong Lewis acidic site can be attributed to the alumina pillars [30-32]. The peak intensity of low temperature desorption peak for Bronsted acidic sites slightly increased with cerium loadings depicting the slight increase in Bronsted acidity, while the intensity of Lewis acidic peak showed very minor changes with increasing cerium loading. The cerium cobalt loaded samples showed minor decrease in acidic property due to the presence of these on the pore opening resulting in the decreased Lewis acidic sites density [29].

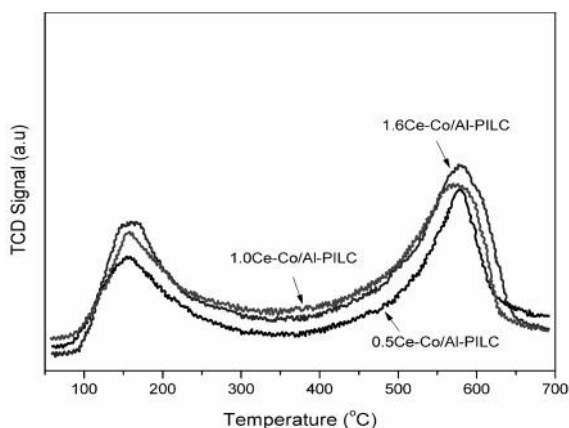


Fig. 2: NH_3 -TPD of the samples.

TPR Studies

The reduction behavior of samples was studied by H_2 -TPR and the obtained TPR profiles are presented in Fig. 3. Normally, the reduction of cobalt oxide occurs in two steps. First step involves the reduction of Co_3O_4 to CoO while in second step CoO undergoes reduction to metallic cobalt (Co^0) [25]. It can be seen from Fig. 3 that the 0.5 wt% cerium modified Co/Al-PILC shows three reduction peaks at 208 °C, 278 °C and 379 °C. The first peak at 208 °C can be attributed to the decomposition of $\text{Co}(\text{NO}_3)_2$ [33]. While peaks at 278 °C and 379 °C may be due to the two step reduction of Co_3O_4 to CoO and CoO to Co^0 , respectively. A distinct change in the TPR profile is observed for higher cerium loaded Co/Al-

PILC, whereas the two steps reduction occurs at 284 °C, 381 °C and at 291 °C, 391 °C for 1 wt% and 1.6 wt% cerium doped catalysts respectively. The shift in reduction peak towards higher temperature confirms the hindrance in Co_3O_4 reduction with cerium addition. Similar trends of TPR profile for cerium promoted Co/SiO_2 was reported by B Ernst et al [21].

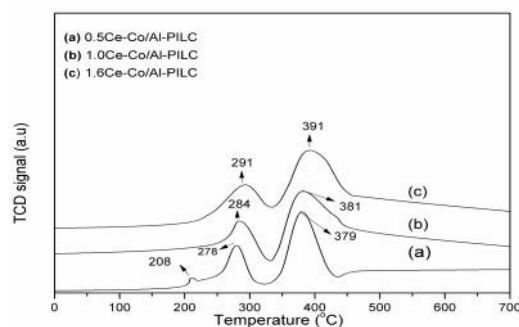


Fig. 3: TPR of the samples.

Thermo Gravimetric Analysis (TGA)

TGA of 20 wt% Co/Al-PILC with different cerium loadings has been carried out (Fig. 4). This is clearly seen from TGA data that all samples exhibit continuous weight lost behavior till 800 °C. The weight lost upto 160 °C can be attributed to the removal of surface adsorbed water while the weight lost between 150 °C to 500 °C is attributed to the interlayer water and due to the dehydroxylation of cerium species. Interestingly, as the wt% of cerium increased, the weight loss around 300 °C also increased. The continuous weight lost from 600 °C till 800 °C was attributable to the removal of hydroxide groups as a result of dehydroxylation of pillar and clay structure, causing collapse in MMT layer structure [10-12, 28, 29, 33-36]. These results also show an agreement with previously reported results for thermal behavior of vanadia-loaded pillared clays [34].

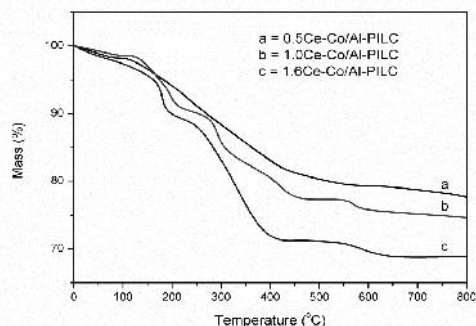


Fig. 4: TGA curves of the samples.

SEM Studies

Fig. 5, presents the typical SEM micrographs of prepared samples. NaMMT and cerium promoted Co/Al-PILC exhibits flake like morphology. It is interesting to note from micrographs that cerium addition and calcination temperature has no marked effect on the layered structure of MMT. No apparent morphology and distribution of cobalt and cerium particles was observed due to densified nature of clay as well as lower magnification of the instruments. In addition, high dispersion and lower concentration of cobalt and cerium hinders the study of surface morphology for these metal particles on MMT clay surface.

Catalytic Activity

Effect of Ce Doping on FT Activity of Co Supported Al-PILC

The effect of Al-pillaring on the FT activity of Co-supported MMT catalysts was reported in our previous findings [4, 9]. In this work, we present the effect of Ce promoter on the FT activity of Al-PILC supported cobalt catalyst. The incorporation of Ce to the Co-supported Al-PILC has pronounced effect on the catalytic activity and product selectivity (Table-3). The CO conversion boosts up to 33.5% resulting in higher selectivity of C_{5+} hydrocarbons over cerium modified Co/Al-PILC. This may be due to the increased dispersion of Co_3O_4 on the surface of support and presence of larger active sites as a result of cerium addition.

Moreover, addition of 1.6 wt% Ce to 20 wt% Co/Al-PILC resulted in the increased selectivity of gasoline range hydrocarbons (C_5-C_{12}) and methane from 18.23% to 31.7% and 27.7 to 30.8%, respectively, while selectivity of C_{21+} were decreased to 23.1%. This behavior can be attributed to the ability of cerium to promote the hydrocracking ability of cobalt supported Al-pillared clay and is in accordance to the results reported for cerium promoted Co/SiO₂ catalysts [21]. The lower catalytic activity was expected due to the increase in reduction temperature of Co_3O_4 after the cerium incorporation. The unexpected increase in initial activity and C_{5+} products selectivity were seen after the reaction which can be attributed to the more active sites as a result of CeO_2 to CeO_{2-x} partial reduction [18-21] on the surface of Co/Al-PILC after cerium doping [17, 19]. In FT synthesis (CH_x)_{ad} species are formed as a result of hydrogenation of adsorbed CO on the surface of catalysts which are mainly responsible for the production of methane via hydrogenation or higher hydrocarbons via polymerization. Furthermore, the hydrogenation of (CH_x)_{ad} suppressed with the incorporation of cerium due to enhanced formation of Co-C intermediates, resulting in decreased (CH_x)_{ad} hydrogenation. The improved FT catalytic activity may also be attributed to the modified electronic properties of Co-atoms as a result of CeO_2 to CeO_{2-x} partial reduction. This behavior is similar to the results reported earlier for cerium promoted Co/SiO₂ catalysts [37].

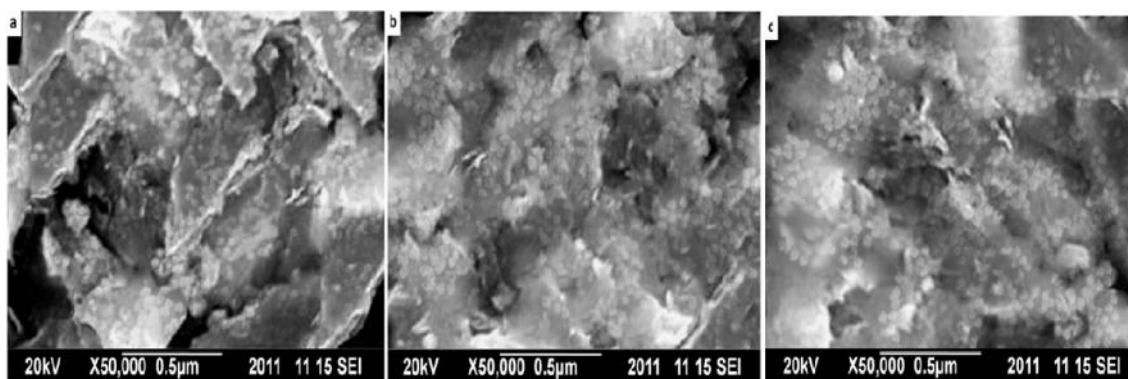


Fig. 5: SEM images (a) 0.5 Ce-Co/Al-PILC (b) 1.0 Ce-Co/Al-PILC (c) 1.6 Ce-Co/Al-PILC.

Table-3: Results of different catalysts for FT synthesis.

Catalysts	CO conversion	CO ₂ selectivity	C ₁ (Wt%)	C ₅ -C ₁₂ (Wt%)	C ₁₃ -C ₂₀ (Wt%)	C ₂₁₊ (Wt%)
20wt% Co/NaMMT	10.0	2.3	40.0	12.5	8.0	37.2
20wt% Co/Al-PILC	28.0	2.5	27.2	18.2	11.0	41.3
0.5 Ce-Co/Al-PILC	31.0	2.0	28.0	21.7	11.7	36.5
1.0 Ce-Co/Al-PILC	33.0	2.3	28.9	26.0	11.3	31.4
1.6 Ce-Co/Al-PILC	33.5	2.4	30.8	31.7	12.0	23.1

The catalyst stability of Co/Al-PILC was studied for reaction time of 30h, initially. The CO conversion was achieved up to 28% for 20 wt% Co/Al-PILC (Fig. 6) which decreased with TOS and reached at minimum level of 11% after 30h of TOS, calculated by a normalization equation [9]. However, the cerium modified catalysts showed higher TOS stability. 0.5 and 1% cerium addition showed little decrease in CO conversion after 8h which remained constant for 30h of TOS while 1.6% cerium catalyst showed higher stability and constant catalytic activity for 30h of TOS. It is obvious from our results that cerium addition to the Co/Al-PILC catalyst increases the catalyst stability and higher cerium loading (1.6 wt%) showed greater TOS stability and is in agreement with previously reported results for Co/SiO₂ system [38]. The catalytic activity of different catalysts were in order of 1.6 wt% Ce-20wt% Co/Al-PILC > 1wt% Ce-20wt% Co/Al-PILC > 0.5wt% Ce-20 wt%Co/Al-PILC > 20wt% Co/Al-PILC. These results prove that, as the cerium loading increases, the degree of dispersion of Co₃O₄ also increases on the surface of Al-PILC and hence catalytic activity increases. This enhanced catalytic activity with the increased cerium modified sample is mainly due to high dispersion ability of cerium over the support.

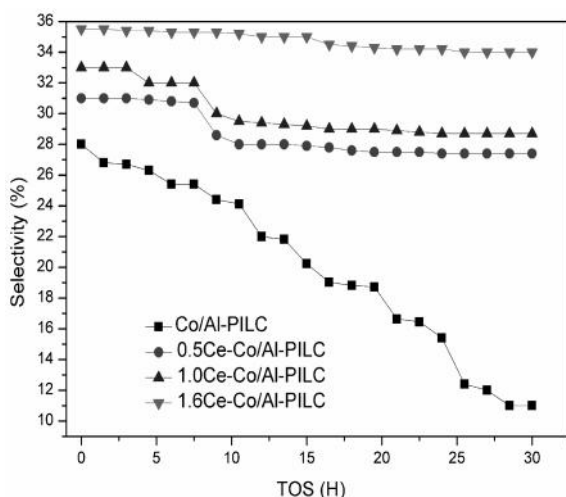


Fig. 6: CO-conversion/selectivity verses time on stream for different wt% Ce-Co/Al-PILC catalysts.

Effect of Reaction Temperature and Pressure on Catalytic Activity of Catalysts

The effect of reaction temperature and reaction pressure on catalytic activity of 1.6 wt% Ce 20 wt% Co/Al-PILC was also investigated and presented in Fig. 7.a and Fig. 7.b respectively.

The reaction carried out at a temperature of 220 °C gives almost 33.5% CO conversion resulting in the hydrocarbons selectivity of 30.8, 31.7, 12 and 23.1% for methane, C₅-C₁₂, C₁₃-C₂₀, C₂₁₊ respectively (Fig. 7.a). When the reaction temperature is increased to 260 °C, the CO conversion and methane selectivity also increased to 35.4 and 32.7, respectively, and decrease in C₅₊ hydrocarbons selectivity to 28.6%. Furthermore, as the temperature is increased to 275 °C, the CO conversion was increased to 36.3% and selectivity of methane to 34% while the C₅₊ hydrocarbons decreased to 28%. However, no significant change in the selectivity of C₁₃-C₂₀ and C₂₁₊ hydrocarbons was observed with increase in reaction temperature. This effect of the catalysts can be attributed to the higher hydrogenation activity of the catalysts at high temperature similar to the performance of standard cobalt-thorium catalysts [39]. Increase in reaction temperature from 220 to 275 °C results in higher production of methane which is not beneficial in Co-based FT synthesis as reported earlier [40]. Reaction pressure also imparts crucial role on the activity and selectivity of FT catalysts.

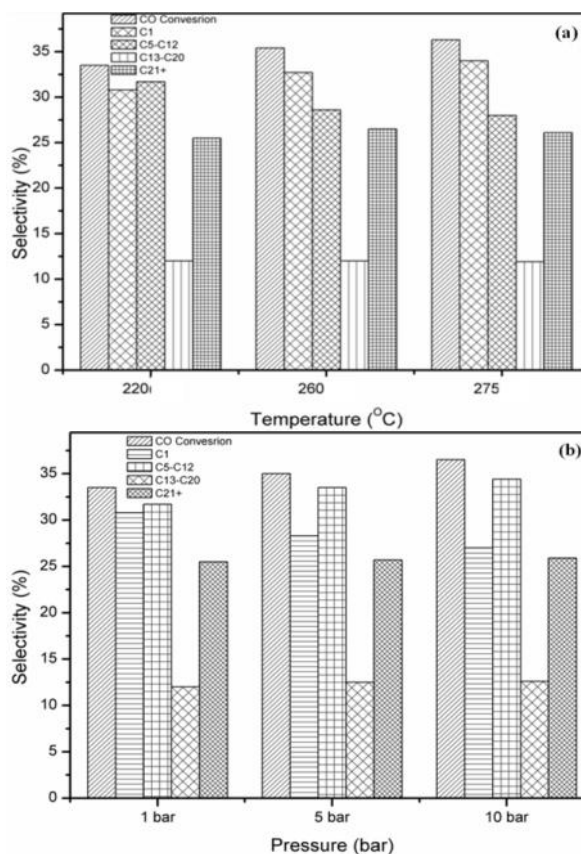


Fig. 7: Effect of reaction temperature (a) and reaction pressure (b) on FT catalytic activity.

The FT reaction carried out at a pressure of 1, 5 and 10 bar is shown in Fig. 7.b. At a pressure of 1 bar, the CO conversion was 33.5%, while selectivity of methane and C₅-C₁₂ hydrocarbons was 30.8% and 31.7%, respectively, over 1.6 wt% Ce-20 wt% Co/Al-PILC. As the pressure is increased from 5 to 10 bar, the CO conversion was increased from 35 to 36.5%, while the methane selectivity was decreased to 28.3 and 27%, respectively. At this increased pressure, the percent selectivity of C₅-C₁₂ hydrocarbons was also improved from 33.5 to 34.4% (Fig. 7.b). A little change in the selectivity of C₁₃-C₂₀ and C₂₁₊ hydrocarbons was observed with increasing reaction pressure. It can be concluded that higher pressure favors the production of high molecular weight hydrocarbons as a result of chain growth probability [41]. The increase in CO conversion can be ascribed to the increase in partial pressure of hydrogen because the reaction rate is proportional to the hydrogen partial pressure and the increased selectivity of the C₅₊ hydrocarbons is due to the increased CO partial pressure [42].

The enhanced catalytic activity and lower methane selectivity was achieved over Al-pillared MMT supported Co catalyst. The Na⁺ in MMT interlayer responsible for higher methane production was completely replaced by Al after pillaring along with enhanced CoO reduction. The incorporation of small amount of cerium to the Co/Al-PILC results in increase in reduction temperature. Instead of increase in reduction temperature cerium incorporation results in high dispersion of cobalt particles and formation of new active sites which are responsible for higher catalytic activity and higher hydrocarbons (C₅-C₁₂) selectivity. The increased selectivity towards methane and C₅-C₁₂ hydrocarbons were obtained over cerium modified Co/Al-PILC as a result of cracking of C₂₂₊ hydrocarbons. The addition of cerium to the Co/Al-PILC increases C₂-C₄ hydrocarbons of FT products due to decreased availability of adsorbed hydrogen. Higher reaction temperature (>220 °C) increases CO conversion and methane selectivity and decreases C₅₊ hydrocarbons selectivity. Increase in reaction pressure from 1 to 10 bar favors an increase in C₅₊ hydrocarbons selectivity and decrease in the methane fraction.

Conclusions

The enhanced catalytic activity and lower methane selectivity was achieved over Al-pillared MMT supported Co catalyst. The Na⁺ in MMT interlayer responsible for higher methane production was completely replaced by Al after pillaring along with enhanced CoO reduction. The incorporation of

small amount of cerium to the Co/Al-PILC results in increase in reduction temperature. Instead of increase in reduction temperature cerium incorporation results in high dispersion of cobalt particles and formation of new active sites which are responsible for higher catalytic activity and higher hydrocarbons (C₅-C₁₂) selectivity. The increased selectivity towards methane and C₅-C₁₂ hydrocarbons were obtained over cerium modified Co/Al-PILC as a result of cracking of C₂₂₊ hydrocarbons. The addition of cerium to the Co/Al-PILC increases C₂-C₄ hydrocarbons of FT products due to decreased availability of adsorbed hydrogen. Higher reaction temperature (>220°C) increases CO conversion and methane selectivity and decreases C₅₊ hydrocarbons selectivity. Increase in reaction pressure from 1 to 10 bar favors an increase in C₅₊ hydrocarbons selectivity and decrease in the methane fraction.

Acknowledgements

Authors would like to thank Higher Education Commission (HEC) of Pakistan for financial support of this work.

References

1. S. Li, S. Krishnamoorthy, A. Li, G. D. Meitzner and E. Iglesia, Promoted Iron-Based Catalysts for the Fischer-Tropsch Synthesis: Design, Synthesis, Site Densities, and Catalytic Properties, *J. Catal.*, **206**, 202 (2002).
2. A. Dinse, M. Aigner, M. Ulbrich, G. R. Johnson and A. T. Bell, Effects of Mn Promotion on the Activity and Selectivity of Co/SiO₂ for Fischer-Tropsch Synthesis, *J. Catal.*, **288**, 104 (2012).
3. S. Zeng, Y. Du, H. Su and Y. Zhang, Promotion Effect of Single or Mixed Rare Earths on Cobalt-Based Catalysts for Fischer-Tropsch Synthesis, *Catal. Commun.*, **13**, 6 (2011).
4. N. Ahmad, S. Hussain, B. Muhammad, T. Mahmood, Z. Ali, N. Ali, S. Abbas, R. Hussain and S. Aslam, Effect of the Reaction Conditions on Al-Pillared Montmorillonite Supported Cobalt-Based Catalysts for Fischer Tropsch Synthesis, *Dig. J. Nanomat. Biostr.*, **8**, 347 (2013).
5. S. T. Hussain, M. Mazhar and M. A. Nadeem, Suppression of Methane Formation During Fisher-Tropsch Synthesis Using Manganese-Cobalt Oxide Supported on H-5A Zeolite as a Catalyst, *J. Nat. Gas Chem.*, **18**, 187 (2009).
6. K. Jalama, N. J. Coville, H. Xiong, D. Hildebrandt, D. Glasser, S. Taylor, A. Carley, J. A. Anderson and G. J. Hutchings, A Comparison of Au/Co/Al₂O₃ and Au/Co/SiO₂

- Catalysts in the Fischer–Tropsch Reaction, *Appl. Catal. A.*, **395**, 1 (2011).
- V. Calemma, S. Peratello and C. Perego, Hydroisomerization and Hydrocracking of Long Chain n-Alkanes on Pt/Amorphous SiO₂–Al₂O₃ Catalyst, *Appl. Catal. A.*, **190**, 207 (2000).
 - X. Dupain, R. A. Krul, M. Makkee and J. A. Moulijn, Are Fischer–Tropsch Waxes Good Feedstocks for Fluid Catalytic Cracking Units, *Catal. Today*, **106**, 288 (2005).
 - N. Ahmad, S. Hussain, B. Muhammad, N. Ali, S. Abbas and Y. Khan, Effect of Manganese Promotion on Al-Pillared Montmorillonite Supported Cobalt Nanoparticles for Fischer–Tropsch Synthesis, *Bull. Korean Chem. Soc.*, **34**, 3005 (2013).
 - H. Su, S. Zeng, H. Dong, Y. Du, Y. Zhang and R. Hu, Pillared Montmorillonite Supported Cobalt Catalysts for the Fischer–Tropsch Reaction, *Appl. Clay Sci.*, **46**, 325 (2009).
 - N. Ahmad, S. T. Hussain, B. Muhammad, N. Ali, S. M. Abbas and Z. Ali, Zr-pillared Montmorillonite Supported Cobalt Nanoparticles for Fischer–Tropsch Synthesis, *Prog. Nat. Sci: Mater. Int.*, **23**, 374 (2013).
 - K. V. Bineesh, S.-Y. Kim, B. R. Jermy and D.-W. Park, Catalytic Performance of Vanadia-Doped Titania-Pillared Clay for the Selective Catalytic Oxidation of H₂S, *J. Ind. Engineer. Chem.*, **15**, 207 (2009).
 - H. Li, S. Wang, F. Ling and J. Li, Studies on MCM-48 Supported Cobalt Catalyst for Fischer–Tropsch Synthesis, *J. Mol. Catal. A.*, **244**, 33 (2006).
 - T. K. Das, G. Jacobs, P. M. Patterson, W. A. Conner, J. Li and B. H. Davis, Fischer–Tropsch Synthesis: Characterization and Catalytic Properties of Rhenium Promoted Cobalt Alumina Catalysts, *Fuel*, **82**, 805 (2003).
 - D. Schanke, S. Vada, E. A. Blekkan, A. M. Hilmen, A. Hoff and A. Holmen, Study of Pt-Promoted Cobalt CO Hydrogenation Catalysts, *J. Catal.*, **156**, 85 (1995).
 - A. Kogelbauer, J. J. G. Goodwin and R. Oukaci, Ruthenium Promotion of Co/Al₂O₃ Fischer–Tropsch Catalysts, *J. Catal.*, **160**, 125 (1996).
 - G. J. Haddad, B. Chen and J. J. G. Goodwin, Effect of La³⁺ Promotion of Co/SiO₂ on CO Hydrogenation, *J. Catal.*, **161**, 274 (1996).
 - G. R. Moradi, M. M. Basir, A. Taeb and A. Kiennemann, Promotion of Co/SiO₂ Fischer–Tropsch Catalysts with Zirconium, *Catal. Commun.*, **4**, 27 (2003).
 - A. Guerrero-Ruiz, A. Sepuñveda-Escribano and I. Rodríguez-Ramos, Carbon Monoxide Hydrogenation Over Carbon Supported Cobalt or Ruthenium Catalysts. Promoting Effects of Magnesium, Vanadium and Cerium Oxides, *Appl. Catal. A.*, **120**, 71 (1994).
 - J. Barrault, A. Guilleminot, J. C. Achard, V. Paul-Boncour and A. Percheron-Guegan, Hydrogenation of Carbon Monoxide on Carbon-Supported Cobalt Rare Earth Catalysts, *Appl. Catal.*, **21**, 307 (1986).
 - B. Ernst, L. Hilaire and A. Kiennemann, Effects of Highly Dispersed Ceria Addition on Reducibility, Activity and Hydrocarbon Chain Growth of a Co/SiO₂ Fischer–Tropsch Catalyst, *Catal. Today*, **50**, 413 (1999).
 - J. Barrault, S. Probst, A. Alouche, A. Percheron-Guegan, V. Paul-Boncour and M. Primet, *Characterization and Catalytic Properties of Nickel Oxide Supported on Rare Earth Oxides. Description of the Metal-Support Interaction*, in *Studies in Surface Science and Catalysis*, Elsevier, p. 357 (1991).
 - Y. Liu, K. Murata, K. Okabe, M. Inaba, I. Takahara, T. Hanaoka and K. Sakanishi, Selective Hydrocracking of Fischer–Tropsch Waxes to High-quality Diesel Fuel Over Pt-promoted Polyoxocation-pillared Montmorillonites, *Top. Catal.*, **52**, 597 (2009).
 - L. S. Cheng and R. T. Yang, Tailoring Micropore Dimensions in Pillared Clays for Enhanced Gas Adsorption, *Micropor. Mater.*, **8**, 177 (1997).
 - G. W. Wang, Q. Q. Hao, Z. T. Liu and Z. W. Liu, Fischer–Tropsch Synthesis Over Co/montmorillonite-Insights Into the Role of Interlayer Exchangeable Cations, *Appl. Catal. A.*, **405**, 45 (2011).
 - B. Jongsomjit, J. Panpranot and J. G. Goodwin Jr, Co-Support Compound Formation in Alumina-Supported Cobalt Catalysts, *J. Catal.*, **204**, 98 (2001).
 - Z. Zsoldos, T. Hoffer and L. Guzzi, Structure and Catalytic Activity of Alumina-Supported Platinum-Cobalt Bimetallic Catalysts. 1. Characterization by X-ray Photoelectron Spectroscopy, *J. Phys. Chem.*, **95**, 798 (1991).
 - Z. Zsoldos and L. Guzzi, Structure and Catalytic Activity of Alumina Supported Platinum-Cobalt Bimetallic Catalysts. Effect of Treatment on the Interface Layer, *J. Phys. Chem.*, **96**, 9393 (1992).
 - K. V. Bineesh, D.-K. Kim, M.-I. L. Kim and D.-W. Park, Selective Catalytic Oxidation of H₂S Over V₂O₅ Supported on TiO₂-pillared Clay Catalysts in the Presence of Water and Ammonia, *Appl. Clay Sci.*, **53**, 204 (2011).

30. S. Awate, S. Waghmode, K. Patil, M. Agashe and P. Joshi, Influence of Preparation Parameters on Characteristics of Zirconia-Pillared Clay Using Ultrasonic Technique and Its Catalytic Performance in Phenol Hydroxylation Reaction, *Kor. J. Chem. Eng.*, **18**, 257 (2001).
31. N. N. Binitha and S. Sugunan, Preparation, Characterization and Catalytic Activity of Titania Pillared Montmorillonite Clays, *Microporous and Mesoporous Mater.*, **93**, 82 (2006).
32. L. Chmielarz, P. Kurowski, M. Zbroja, A. Rafalska-Lasocha, B. Dudek and R. Dziembaj, SCR of NO by NH₃ on Alumina or Titania-Pillared Montmorillonite Various Modified with Cu or Co: Part I. General Characterization and Catalysts Screening, *Appl. Catal. B: Environ.*, **45**, 103 (2003).
33. Q. Borg, S. Eri, E. A. Blekkan, S. Storsæter, H. Wigum, E. Rytter and A. Holmen, Fischer-Tropsch Synthesis Over γ -Alumina-Supported Cobalt Catalysts: Effect of Support Variables, *J. Catal.*, **248**, 89 (2007).
34. K. V. Bineesh, D. K. Kim, D. W. Kim, H. J. Cho and D. W. Park, Selective Catalytic Oxidation of H₂S to Elemental Sulfur Over V₂O₅/Zr-Pillared Montmorillonite Clay, *Energy Environ. Sci.*, **3**, 302 (2010).
35. P. Cañizares, J. L. Valverde, M. R. Sun Kou and C. B. Molina, Synthesis and Characterization of PILCs With Single and Mixed Oxide Pillars Prepared From Two Different Bentonites. A Comparative Study, *Microporous and Mesoporous Mater.*, **29**, 267 (1999).
36. K. V. Bineesh, D. K. Kim, H. J. Cho and D. W. Park, Synthesis of Metal-Oxide Pillared Montmorillonite Clay For The Selective Catalytic Oxidation of H₂S, *J. Ind. & Eng. Chem.*, **16**, 593 (2010).
37. X. Dai, C. Yu, R. Li, H. Shi and S. Shen, Role of CeO₂ Promoter in Co/SiO₂ Catalyst for Fischer-Tropsch Synthesis, *Chin. J. Catal.*, **27**, 904 (2006).
38. X. Dai, C. Yu and R. Li, Deactivation of CeO₂-Promoted Co/SiO₂ Fischer-Tropsch Catalysts, *Chin. J. Catal.*, **28**, 1047 (2007).
39. S. Colley, R. G. Copperthwaite, G. J. Hutchings and M. Van der Riet, Carbon Monoxide Hydrogenation Using Cobalt Manganese Oxide Catalysts: Initial Catalyst Optimization Studies, *Ind. & Eng. Chem. Res.*, **27**, 1339 (1988).
40. D. Das, G. Ravichandran and D. K. Chakrabarty, Synthesis of Light Alkenes From Syngas on Silicalite-1 Supported Cobalt and Cobalt-Manganese Catalysts, *Appl. Catal. A.*, **131**, 335 (1995).
41. Z. Yan, Z. Wang, D. B. Bukur and D. W. Goodman, Fischer-Tropsch Synthesis on a Model Co/SiO₂ Catalyst, *J. Catal.*, **268**, 196 (2009).
42. H. Schulz and M. Claeys, Kinetic Modelling of Fischer-Tropsch Product Distributions, *Appl. Catal. A.*, **186**, 91 (1999).